Advances in Bridge Engineering

ORIGINAL INNOVATION Open Access

Numerical analysis on the time-varying temperature field distribution patterns of ballastless track steel-concrete composite box girders at ambient temperature based on field measurements

Wangqing Wen[1], Shiwei Li[1,2*], Aiguo Yan[1] and Jiahua Zeng[1]

* Correspondence: lishiwei1987@my.swjtu.edu.cn
[1]China Railway Siyuan Survey and Design Group Company Limited, Wuhan 430063, China
[2]Southwest Jiaotong University, Chengdu 610031, China

Abstract

To analyze the time-varying temperature field distribution pattern of ballastless track steel-concrete composite box girders for a high-speed railway at ambient temperature, a numerical model for analyzing the time-varying temperature field of steel-concrete composite box girders was established based on the long-term monitoring data for the internal and external environments of the main girder of the Ganjiang Bridge on the Nanchang-Ganzhou high-speed railway. The influence of factors such as the deck pavement and the ambient wind speed on the time-varying temperature field of the steel-concrete composite box girders were considered. The results showed that there was a significant difference in the vertical temperature gradient patterns on sections at the side web and at the middle web at the same moment in time due to the hindering effect of the track board on the heat exchange between the ambient temperature and the main girder. Increasing the wind speed accelerated the rate of heat exchange between the main girder surface and the environment. In particular, when the internal temperature of the girder was higher than the ambient temperature, the higher the wind speed was, the larger the temperature gradient was. This study lays a foundation for accurate analysis of the structural response of ballastless track steel-concrete composite girder bridges at ambient temperature.

Keywords: Steel-concrete composite box girder, Ballastless track, Time-varying temperature field, Ambient temperature, Wind speed

1 Introduction

Steel-concrete composite bridges fully utilize the mechanical properties of the materials. These bridges have lower self-weight and better seismic performance than concrete girders, and they avoid the fatigue cracking problem encountered in the orthotropic plates of steel girders, thereby making them widely used in railroad engineering with broad application prospects (Nie et al. 2012). However, the thermomechanical properties of steel and concrete differ significantly: Steel has a specific heat capacity equal to half that of concrete and a heat transfer coefficient approximately 50 times that of concrete. As a result, the nonuniform distribution of the temperature field inside a steel-concrete composite girder can generate self-restraint thermal stresses during ambient temperature changes and solar radiation (Chang and Im 2010; Zhang et al. 2020). For hyperstatic structures such as continuous beams, secondary thermal stresses may also occur. It has been shown that the temperature effect on hyperstatic bridge structures can reach or even exceed the effect of a live load of vehicle (Abid et al. 2020; Berwanger and Symko 1975; Giussani 2009). Therefore, it is important to accurately analyze the time-varying temperature field distribution pattern and structural response of steel-composite girder bridges at ambient temperature.

The existing studies have been focused on the investigations of the temperature field distribution patterns of highway steel-concrete composite girders, with the vertical temperature gradients on the composite girder sections obtained through a combination of field measurements and theoretical analyses. For example, in 1977, Emerson (1977) carried out temperature measurement on a highway steel-concrete composite girder for a period of 16 days and proposed a mathematical model for the vertical temperature gradient on the composite girder section. In 1987, Kennedy and Soliman (1987) proposed a simple mathematical model for a vertical temperature gradient based on the temperature field measurement data for an I-shaped steel-concrete composite girder. Liu et al. (2019) carried out field measurements of the temperature field evolution at the mid span of the main girder of the Haihuang Bridge, a highway steel-concrete composite girder cable-stayed bridge with a main span of 560 m, over a period of nearly a year, and they analyzed the evolution of the vertical temperature gradient on the main girder section. For the composite box girders with railway ballastless track arranged on the bridge deck, the thickness of the nonuniform track boards reached or even exceeded that of the concrete slab. Considering the characteristics of high levels of solar radiation and low rainfall in Nevada, USA, Lawson et al. (2020) statistically analyzed the continuous temperature monitoring data, and based on the data, they pointed out that a design using the values in AASHTO specifications (AASHTO 2010) would make bridge structures unsafe. Abid et al. (2018) experimentally studied the temperature field distribution of composite girders undergoing alternating hot and cold seasons, and they pointed out that the thickness of the concrete slab significantly affected the temperature field distribution. Therefore, the characteristics of the bridge deck structure of a ballastless track composite box girder need to be specifically investigated to accurately understand its temperature field distribution pattern. In addition, the field distribution pattern of a composite box girder, the interior of which is always a relatively confined environment, differs significantly from that of an open I-shaped steel-concrete composite girder.

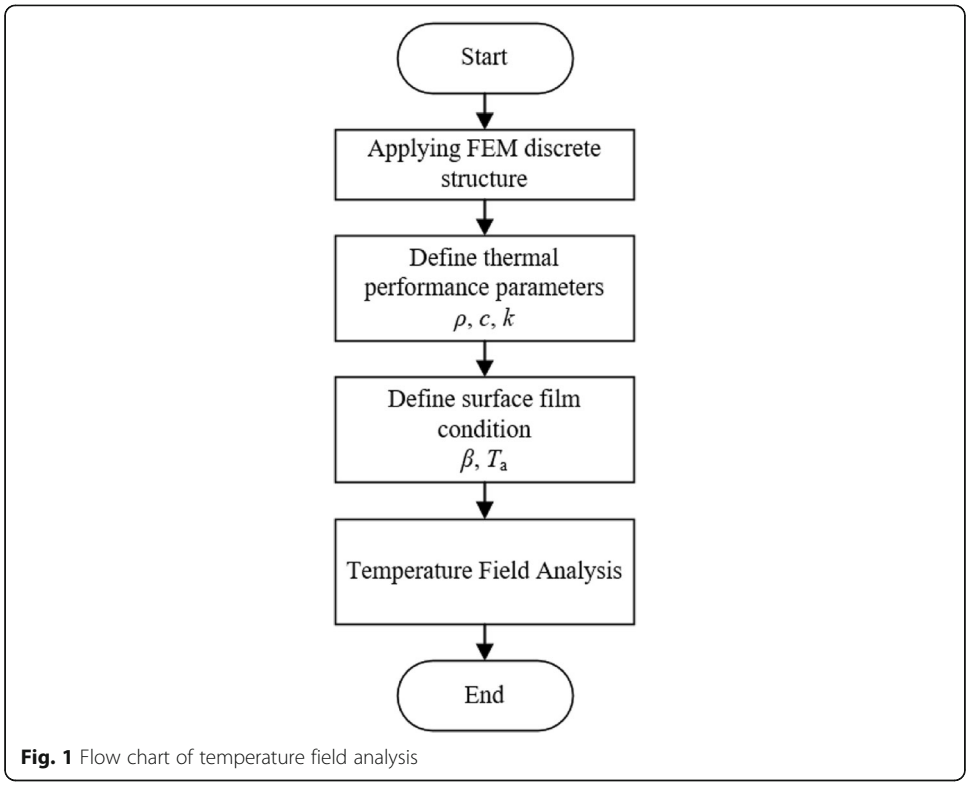

Fig. 1 Flow chart of temperature field analysis

In this study, the world's largest-span steel-concrete composite girder cable-stayed bridge, i.e., the Ganjiang Bridge on the Nanchang-Ganzhou high-speed railway, was taken as an example, a numerical model for analyzing the time-varying temperature field of steel-concrete composite girders was established with consideration of the influence of the deck pavement and the ballastless track structure based on a statistical analysis of the field measurements of the main girder of this bridge for nearly a year. Using this model, the effects of factors such as the deck pavement and the ambient wind speed on the time-varying temperature field of steel-concrete composite box girders were investigated, the distribution patterns of the time-varying temperature fields of steel-concrete composite girders for ambient temperature and different wind speeds were analyzed, and the calculated results were compared with the values of the current code specifications.

The actual temperature field of a bridge structure is related to factors such as the ambient temperature, solar radiation intensity, wind speed, location, and orientation of the bridge (Oskar and Sven 2011; Zhou and Yi 2013; Saetta et al. 1995; Abid et al. 2016; Song et al. 2012; Xue et al. 2018). In view of the complexity of this problem, in this study, the effect of the ambient temperature change on the temperature field of steel-concrete composite girders was mainly analyzed.

2 Numerical model and validation

2.1 Analysis model

According to the principle of thermal equilibrium, the heat absorbed due to an increase in the structural temperature is equal to the external inflow heat, the differential equation for temperature conduction can be expressed as

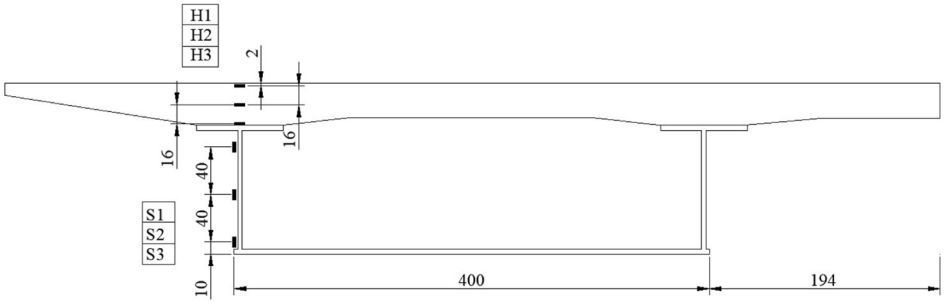

Fig. 2 Main girder section temperature measuring points (units: cm)

$$\rho c \frac{\partial T}{\partial \tau} = k \nabla^2 T \tag{1}$$

Here, k is thermal conductivity; c is specific heat; ρ is density; τ is time; T is temperature.

On the interface between steel and concrete, it can be assumed that the temperature and heat flux are continuous, and the boundary condition can be expressed as (Zhu 2012)

$$T_s = T_c, -k_s\left(\frac{\partial T_s}{\partial n}\right) = k_c\left(\frac{\partial T_c}{\partial n}\right) \tag{2}$$

Here, k_c and k_s are thermal conductivity of concrete and steel respectively; n is the normal outside the interface.

When steel or concrete is in contact with air, it can be assumed that the heat flux on the surface of the structure is proportional to the difference between the surface temperature T and the air temperature T_a, and the boundary condition can be expressed as (Zhu 2012)

$$-k\left(\frac{\partial T}{\partial n}\right) = \beta(T - T_a) \tag{3}$$

Here, β is the surface conductance.

The surface heat transfer coefficient of the box girder was calculated using the method of calculating the interfacial convective heat transfer coefficient obtained by

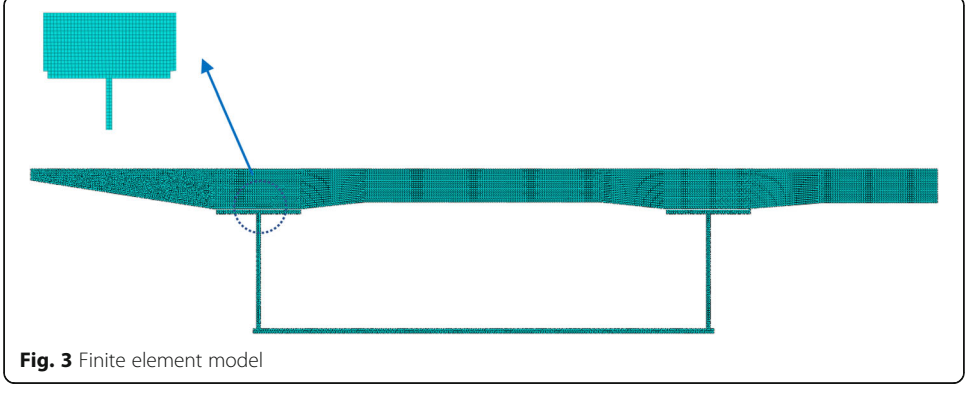

Fig. 3 Finite element model

Table 1 Values of thermal performance parameters of steel and concrete

	Specific heat capacity c J/(kg.°C)	Thermal conductivity k W/(m.°C)	Density ρ kg/m^3
Concrete	1000	1.56	2438
Steel	475	58.5	7500

Zhang and Liu (2006) based on wind tunnel tests, as shown in Eq. (4). The wind speed inside the box girder could be approximated as 0 m/s.

$$\beta = 3.06v + 9.55 \tag{4}$$

where v is the wind speed, in m/s, and β has the units of W/(m^2.°C).

The flow chart of temperature field analysis is shown in Fig. 1.

2.2 Program validation

The accuracy of the proposed method is verified by the measured results of temperature field of a steel-concrete composite girder bridge under sudden change of temperature. It's a simply supported beam with a span of 35 m, the section size of main girder and the location of measuring points are shown in Fig. 2, and other details can be seen in reference (Zhou et al. 2013). Based on the general finite element software ABAQUS, the finite element analysis model is established, as shown in Fig. 3. Both concrete and steel are simulated by the heat conduction element DC2DC4, the test value of Measuring point H1 is used for the upper surface temperature of concrete slab, and the ambient temperature is used for the lower surface temperature of concrete slab and steel beam. The values of the thermal performance parameters of the concrete and steel are reported in Table 1. The comparison between the calculated results and the measured values is shown in Fig. 4. The results show that the proposed method can accurately analyze the internal temperature field of steel-concrete composite girder bridge.

3 Project background and field temperature monitoring program

Ganjiang Bridge, the world's largest-span high-speed railway ballastless track steel-concrete composite girder cable-stayed bridge with a span arrangement of 35.7 + 40 + 60 + 300 + 60 + 40 + 35.7 m, was segmentally constructed in 2018, as

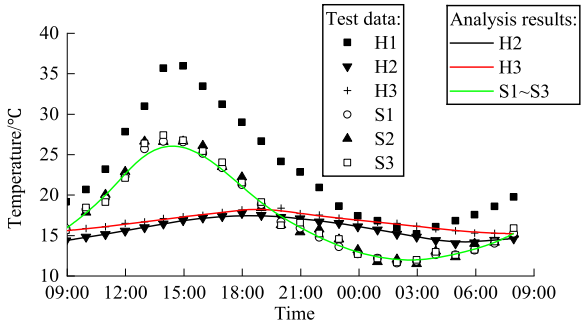

Fig. 4 Comparison between analysis results and measured data

Fig. 5 Ganjiang Bridge on the Nanchang-Ganzhou railway

shown in Fig. 5. The bridge adopts CRTS III slab ballastless track and it has a design speed of 350 km/h. The cross section consists of triple-cells box girder with a total transverse width of 16.3 m, the girder depth is 4.5 m, the concrete slab thickness varies from 0.3 m to 0.5 m, the thickness of the side and middle web of steel girder are 24 mm and 30 mm respectively, the thickness of the bottom plate is 20 mm, the thickness of the U-shaped and I-shaped stiffener are 8 mm and 20 mm respectively, and the specification of the stud is Φ 22 × 200, as shown in Fig. 6. The bridge was opened to traffic in December 2019. To investigate the influence of ambient temperature changes on the temperature field of the main girder, devices for the real-time monitoring of the ambient temperature were installed inside and outside the composite box girder at the mid span of the main girder, as shown in Fig. 7.

In this study, the temperature monitoring data in the time period from 0:00 on September 2, 2019 to 23:00 on October 8, 2020 were extracted. The test data were

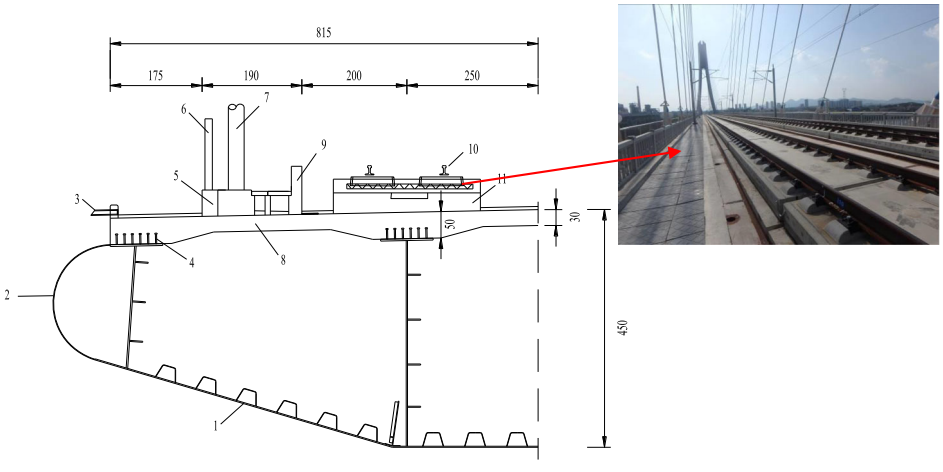

Fig. 6 Schematic diagram of the main girder section (units: cm). 1 steel box girder; 2 wind fairing; 3 water drain pipe; 4 shear connector; 5 vertical wall; 6 railing; 7 contact net frame; 8 concrete slab; 9 protecting wall; 10 rail; 11 track board

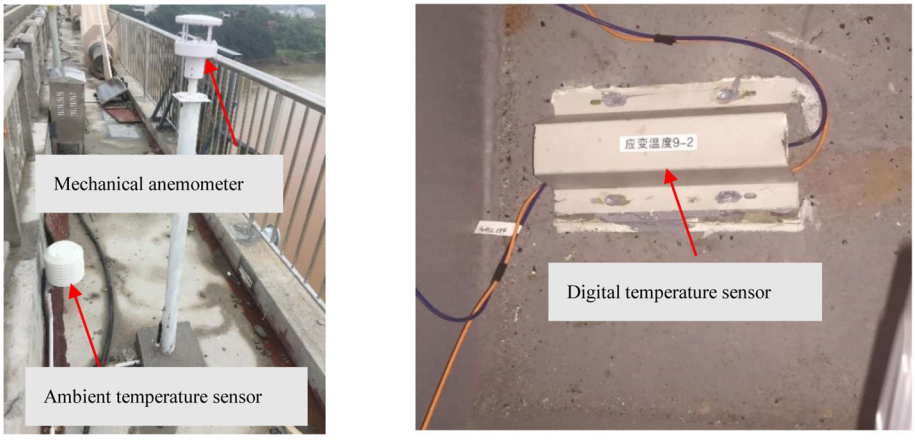

(a) Outside of main girder (b) Inside of main girder

Fig. 7 Ambient temperature acquisition device

collected once per hour for a total of 9670 h, as shown in Fig. 8. The highest and lowest ambient temperatures outside the composite girder were 43.1 °C and 2.8 °C, respectively, and the highest and lowest temperatures inside the composite girder were 34.9 °C and 8.9 °C, respectively. Since the interior of the box girder was in a relatively confined space, the change in the internal temperature of the box girder always lagged behind the change in the external ambient temperature.

4 Finite element analysis model

The geometry of a bridge determines the significant two-dimensional (2D) characteristics of its internal temperature field conduction. In view of this, to analyze the internal temperature field distribution pattern of the composite girders, a numerical analysis model for the sectional 2D thermal conduction was established using the general finite element software ABAQUS. The model considered the influence of the deck appendages (e.g., track board, deck mat, and railing base, as shown in Fig. 9) on the temperature conduction.

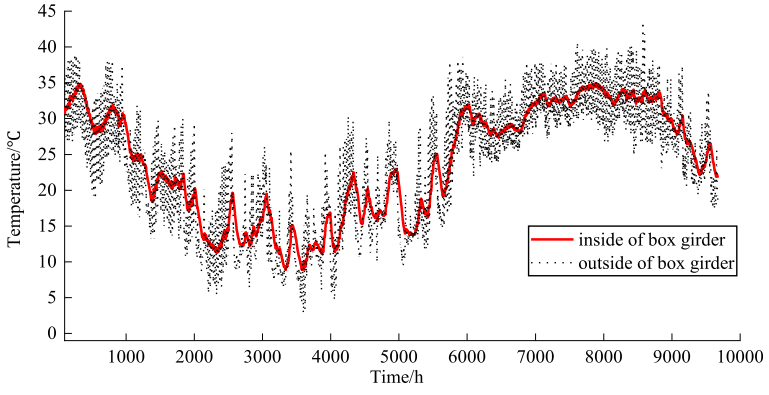

Fig. 8 Changes of temperature inside and outside of the steel-concrete composite box girder (September 2, 2019 to October 8, 2020)

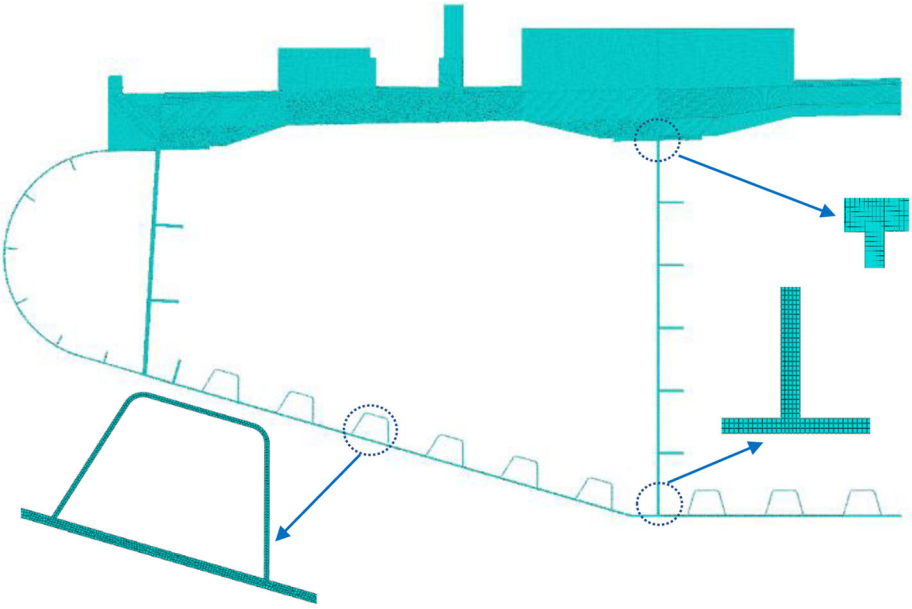

Fig. 9 Finite element model for the temperature field analysis of the composite girder section

Both the concrete slabs and the steel girders were meshed using the heat conduction element DC2DC4 with a maximum element mesh size of 5 mm, resulting in a total of 295,000 elements for the section. An implicit algorithm was used to solve the problem. The surface conductance and the ambient temperature were defined by surface film condition. The finite element analysis model for the temperature field of the composite girder section is shown in Fig. 9. The time step was set to 1 h, with a total of 9670 steps.

The values of thermal performance parameters of the concrete were determined according to the test results of the reserved specimens during construction, while the values of the thermal performance parameters of the steel were relatively stable. The values of the thermal performance parameters of the concrete and steel are reported in Table 2.

The wind speed outside the box girder was found to be in the range of 0 m/s to 9 m/s according to the measured data. Four calculation conditions were established according to the different wind speeds (0 m/s, 3 m/s, 6 m/s, 9 m/s) in order to consider the influence of the external wind speed on the internal temperature field distribution pattern of the composite girder. The bridge was closed in the early morning of August 31, 2019, when the ambient temperature was 24 °C. Therefore, the initial temperature of the composite steel box girder section could be assumed to be 24 °C.

Table 2 Values of thermal performance parameters of steel and concrete

	Specific heat capacity c J/(kg.°C)	Thermal conductivity k W/(m.°C)	Density ρ kg/m^3
Concrete	1000	1.28	2459
Steel	475	58.5	7500

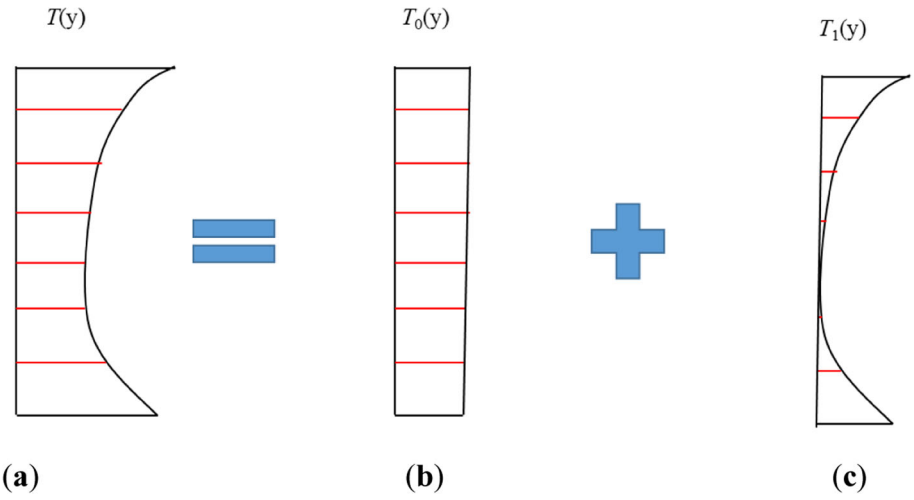

Fig. 10 Method for describing the temperature field of the composite girder section: **a**, **b** Uniform component; **c** Thermal gradient

5 Results and discussion

To describe the distribution pattern of the temperature field of steel-concrete composite box girders, the temperature of the box girder section is usually decomposed into the overall temperature change and the vertical temperature gradient, as shown in Fig. 10.

5.1 Uniform temperature rise and drop

As shown in Fig. 11, the extreme values of the overall temperature drop and rise were − 15 °C and 10.8 °C, respectively.

As mentioned earlier, the interior of the box girder was in a relatively inclosed environment, so the internal temperature change always lagged behind the external temperature change. The temperature nephogram of the composite girder at different moments in time are shown in Fig. 12. There was a small temperature change in the middle region of the web of the box girder, while the top and bottom plates of the box girder had intense heat exchange with the ambient environment. The difference

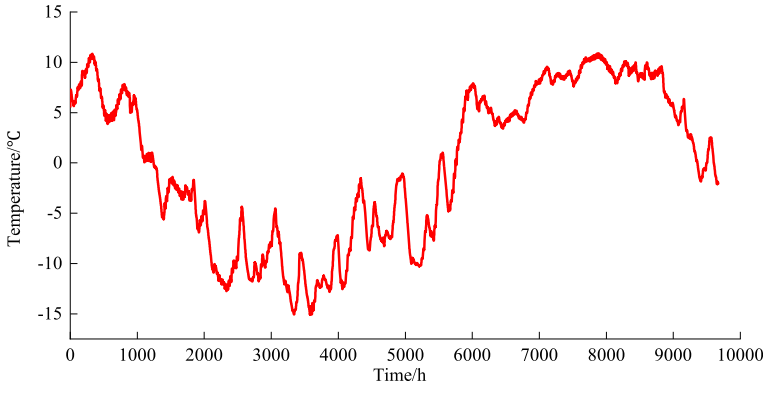

Fig. 11 Temperature difference between the vertical middle region of the web of the composite girder and the closure temperature

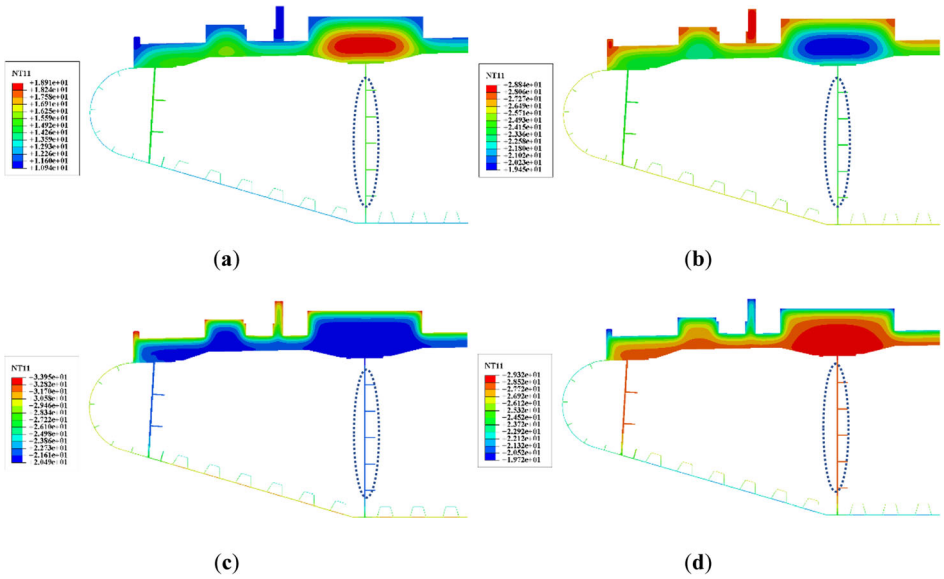

Fig. 12 Temperature distribution nephogram of the composite girder section: **a** t = 05:00, Mar. 31, 2020; **b** t = 16:00, Apr. 18, 2020; **c** t = 16:00, Apr. 18, 2020; and **d** t = 22:00, Sep. 24, 2019. Wind speed = 3 m/s, temperature unit: ℃

between the temperature of the middle region of the web and the closure temperature was precisely the value range of the overall temperature change of the box girder.

5.2 Sectional temperature gradient

Four extreme cases of temperature gradients were extracted from the finite element analysis results, namely, the maximum positive and negative temperature difference between the top concrete slab and the steel web, and the maximum positive and negative temperature difference between the steel beam bottom plate and the web. The temperature nephogram of the composite girder section at a wind speed of 3 m/s is shown in Fig. 12. The calculated values of the typical temperature gradients of the

Table 3 Calculated values of typical temperature gradients in the middle and side webs under different working conditions

t (h)	Wind speed (m/s)	Middle web		Side web	
		ΔT_1(℃)	ΔT_2(℃)	ΔT_1(℃)	ΔT_2(℃)
22:00, Sep. 24, 2019	0	1.2	−3	−5	−2.4
	9	0.9	−5.2	−7.8	− 5
05:00, Mar. 31, 2020	0	4.4	−1.1	−2.5	−0.9
	9	3.9	−2.01	−3.2	−1.8
16:00, Apr. 18, 2020	0	−5	1.0	2.3	0.9
	9	−4.5	2.01	3.0	1.6
08:00, Apr. 27, 2020	0	−1.1	6.3	7.2	3.5
	9	−1.1	8.2	10.9	6.3

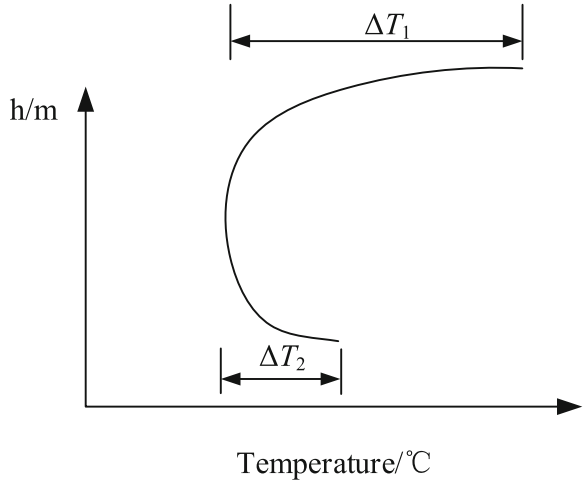

Fig. 13 Typical temperature gradients

middle and side webs under each working condition are shown in Table 3. The meaning of ΔT_1 and ΔT_2 is shown in the Fig. 13.

The results show that there was a significant difference in the vertical temperature gradient for the sections at the side web and the middle web at the same moment in time. For example, Fig. 14 shows the vertical temperature gradient for the section at the middle and side web at t = 05:00, Mar. 31, 2020, when the positive temperature difference between the top concrete slab and the steel web was the largest. However, the temperatures of both the top and bottom slabs at the side web were lower than the temperature of the web at that moment in time, and the temperature field distributions at other moments in time were similar, as shown in Figs. 15, 16 and 17. This phenomenon was mainly due to the fact that the track board above the middle web severely hindered the heat exchange between the top concrete slab of the steel-concrete composite box girder and the atmosphere, while the top and the sides of the top concrete slab at the side web were in direct contact with the atmosphere and hence had a faster heat exchange rate.

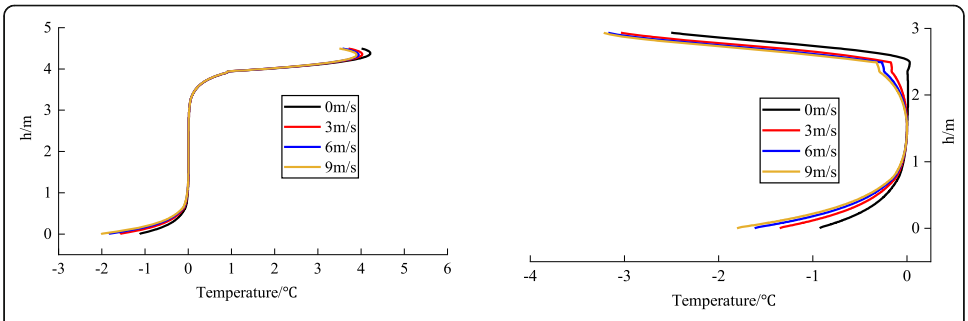

(a) the middle web **(b)** the side web

Fig. 14 Vertical temperature gradient (t = 05:00, Mar. 31, 2020)

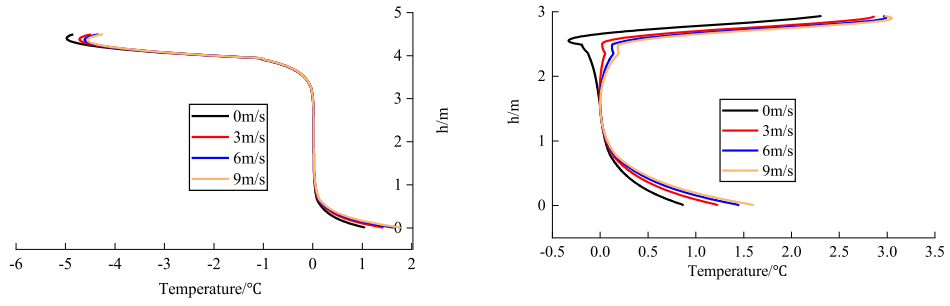

Fig. 15 Vertical temperature gradient (t = 16:00, Apr. 18, 2020)

An analysis of Fig. 17 showed that increasing the wind speed accelerated the rate of heat exchange between the surface of the steel-concrete composite box girder and the environment. Specifically, when the internal temperature of the girder was higher than the ambient temperature, the higher the wind speed was, the more intense the temperature gradient was that was generated at the girder section. For example, at t = 551 h and a wind speed of 0 m/s, the temperature difference ΔT_1 between the top slab and the web was − 5 °C; at a wind speed of 9 m/s, ΔT_1 became − 7.8 °C, which increased by approximately 56%.

In addition, a comparison of Fig. 16(b) and Fig. 17(b) revealed that at ambient temperature, the existence of the temperature difference between the inside and the outside of the box girder not only led to a large temperature difference between the top slab and the web but also resulted in a large temperature gradient between the web and the bottom slab.

The vertical temperature gradients described above were compared with the values from the Eurocode 4 Design of composite steel and concrete structures (BS EN 1994-1-2 2005), as shown in Figs. 18 and 19.

The results showed that for the Ganjiang Bridge, the maximum positive temperature difference between the top slab and the web at the middle web was 4.4 °C, and the maximum positive temperature difference between the top slab and

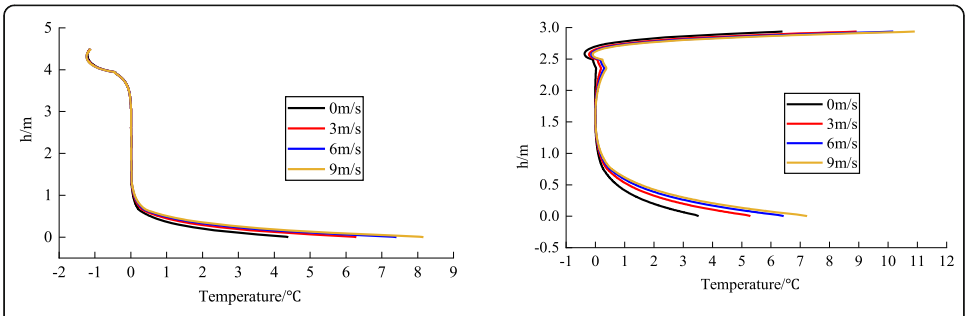

Fig. 16 Vertical temperature gradient (t = 08:00, Apr. 27, 2020)

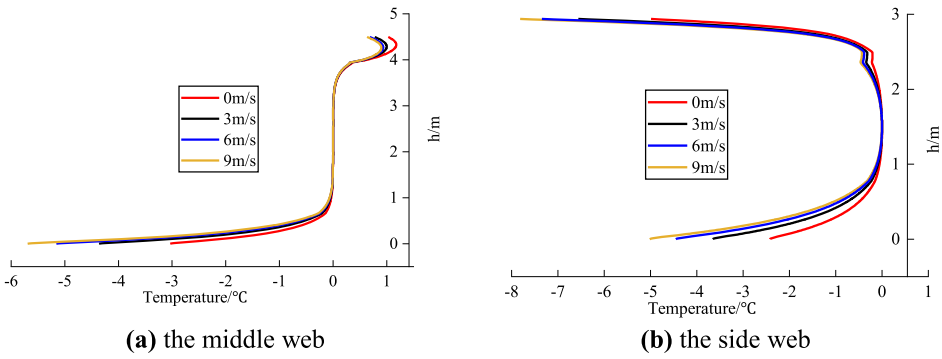

Fig. 17 Vertical temperature gradient (t = 22:00, Sep. 24, 2019)

the web at the side web was 10.9 °C. Both of these values were smaller than the calculated value of 16 °C in the Eurocode. This was mainly because this study was focused on the effect of the ambient temperature change on the temperature field distribution pattern of the main girder without considering the warming effect of the solar radiation on the top slab.

The maximum negative temperature difference between the top slab and the web at the middle web was 5.0 °C. The calculation results are not given here because the values according to the Eurocode provisions on negative temperature gradients differed greatly from the actual values, as shown in Fig. 20. It is worth noting that the current code only specifies the calculation method for the temperature difference between the top slab and the web of a composite girder, but it does not specify how to deal with the difference between the bottom slab and the web of a steel box girder.

6 Conclusions

In this study, a time-varying temperature field analysis model for composite box girders was established based on the long-term field monitoring data of the temperature field of the main girder of the Ganjiang Bridge on the Nanchang-Ganzhou railway, and the effects of the ballastless track deck pavement and the ambient wind speed on the time-

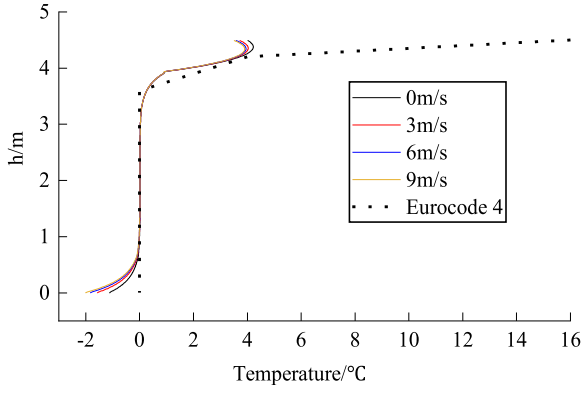

Fig. 18 Comparison of the vertical temperature gradient on a section at the middle web with the code values (t = 5070 h)

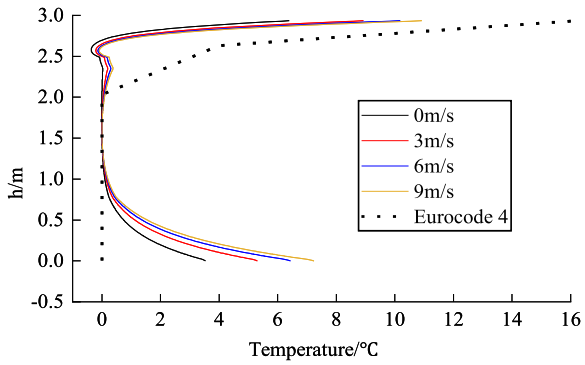

Fig. 19 Comparison of the vertical temperature gradient on a section at the side web with the code values ($t = 5721$ h)

varying temperature field of composite box girders were analyzed. The following conclusions were drawn based on the results presented in this study:

(1) At ambient temperature, the existence of the temperature difference between the inside and the outside of the steel-concrete composite box girder led to temperature gradients not only between the top slab and the web but also between the web and the bottom slab. However, the current code does not provide corresponding provisions for the positive and negative temperature gradients of a bottom slab.
(2) The track board had an important influence on the temperature field distribution pattern of the steel-concrete composite box girders. In particular, for the single-box multi-cell steel-concrete composite box girders, which had multiple webs, there was a significant difference in the vertical temperature gradient pattern of the sections at the side web and the middle web at the same moment in time due to the hindering effect of the track board on the heat exchange between the ambient temperature and the main girder.
(3) Increasing the wind speed accelerated the rate of heat exchange between the surface of the steel-concrete composite box girder and the environment. In particular, when the internal temperature of the girder was higher than the ambient

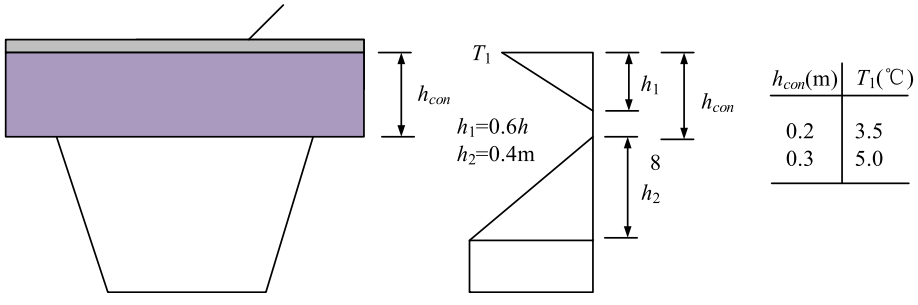

Fig. 20 Eurocode 4 provisions on the calculation of the negative temperature gradient for a composite girder

temperature, the higher the wind speed was, the larger the temperature gradient that was generated at the girder section was.

(4) This study was focused on the effects of ambient temperature change and wind speed on the change pattern of the 3D time-varying temperature field of steel-concrete composite box girders with ballastless track. Further research on the effect of solar radiation is needed.

Abbreviation

CRTS: China Railway Track System

Acknowledgments

This research was supported by Research and development project of China National Railway Group Co., Ltd. (grant number K2018G017 and K2018G018) and China Postdoctoral Science Foundation (grant number 2020 M672460). All these financial supports are greatly appreciated.

Authors' contributions

Conceptualization, W.Q. Wen and S.W. Li; methodology, S.W. Li; software, S.W. Li; validation, A.G. Yan; formal analysis, W.Q. Wen; investigation, S.W. Li; resources, S.W. Li.; data curation, J.H. Zeng; writing—original draft preparation, S.W. Li; writing—review and editing, W.Q. Wen; visualization, S.W. Li; supervision, A.G. Yan; project administration, A.G. Yan; funding acquisition, W.Q. Wen. All authors have read and agreed to the published version of the manuscript. All authors read and approved the final manuscript.

Funding

This research was funded by Research and development project of China National Railway Group Co., Ltd. (grant number K2018G017 and K2018G018) and China Postdoctoral Science Foundation (grant number 2020 M672460).

Availability of data and materials

The data presented in this study are available on request from the corresponding author.

Declaration

Competing interests

The authors declare no conflict of interest.

Received: 22 March 2021 Accepted: 11 May 2021
Published online: 25 May 2021

References

AASHTO (2010) LRFD bridge design specifications. 5th ed. AASHTO, Washington, DC

Abid SR, Mussa F, Taysi N, Ozakca M (2018) Experimental and finite element investigation of temperature distributions in concrete–encased steel girders. Struct Control Hlth 25(1):e2042. https://doi.org/10.1002/stc.2042

Abid SR, Tayi N, Zaka M (2016) Experimental analysis of temperature gradients in concrete box-girders. Construct Build Mater 106(Mar.1):523–532

Abid SR, Tayi N, Zaka M (2020) Temperature records in concrete box-girder segment subjected to solar radiation and air temperature changes. IOP Conf Ser: Mater Sci, Eng 870:012074 (16)

Berwanger C, Symko Y (1975) Thermal stresses in steel–concrete composite bridges. Can J Civ Eng 2(1):66–84. https://doi.org/10.1139/l75-007

BS EN 1994-1-2 (2005) Euro code 4: Design of composite steel and concrete structures. British Standards Institution, London

Chang SP, Im CK (2010) Thermal behavior of composite box-girder bridges. Struct Build 140:117–126

Emerson M (1977) Temperature differences in bridges: basis of design requirements

Giussani F (2009) The effects of temperature variations on the long-term behaviour of composite steel–concrete beams. Eng Struct 31(10):2392–2406. https://doi.org/10.1016/j.engstruct.2009.05.014

Kennedy JB, Soliman MH (1987) Temperature distribution in composite bridges. J Struc Eng 113(3):475–482. https://doi.org/10.1061/(ASCE)0733-9445(1987)113:3(475)

Lawson L, Ryan KL, Buckle IG (2020) Bridge temperature profiles revisited: thermal analyses based on recent meteorological data from Nevada. J Bridg Eng 25:04019111

Liu J, Liu Y, Jiang L, Zhang N (2019) Long-term field test of temperature gradients on the composite girder of a long-span cable-stayed bridge. Adv Struct Eng 22(13):2785–98

Nie JG, Tao MX, Wu LL, Nie X, Li FX, Lei FL (2012) Advances of research on steel-concrete composite bridges. China Civ Eng J 06:110–122

Oskar L, Sven T (2011) Estimating extreme values of thermal gradients in concrete structures. Mater Struct 44:1491–1500

Saetta A, Scotta R, Vitaliani R (1995) Stress analysis of concrete structures subjected to variable thermal loads. J Struc Eng 121(3):446–457. https://doi.org/10.1061/(ASCE)0733-9445(1995)121:3(446)

Song Z, Xiao J, Shen L (2012) On temperature gradients in high-performance concrete box girder under solar radiation. Adv Struct Eng 15(3):399–416. https://doi.org/10.1260/1369-4332.15.3.399

Xue J, Lin J, Briseghella B, Tabatabai H, Chen B (2018) Solar radiation parameters for assessing temperature distributions on bridge cross-sections. Appl Sci 8(4):627. https://doi.org/10.3390/app8040627

Zhang CY, Liu YJ, Liu J, Yuan ZY, Zhang GJ, Ma ZY (2020) Validation of long-term temperature simulations in a steel-concrete composite girder. Struct. 27:1962–1976. https://doi.org/10.1016/j.istruc.2020.07.070
Zhang JR, Liu ZQ (2006) A study on the convective heat transfer coefficient of concrete in wind tunnel experiment. China Civ Eng J 39:39–42
Zhou GD, Yi TH (2013) Thermal load in large-scale bridges: a state-of-the-art review. Int J Distrib Sens N 161:85–93
Zhou YC, Hu SN, Song L, Li ZQ (2013) Effect analysis of steel-concrete composite beam caused by sudden change of temperature. J Traff Trans Eng 13(1):20–26
Zhu BF (2012) Thermal stresses and temperature control of mass concrete. Tsinghua University Press, Beijing, pp 13–30

Publisher's Note